Quantum Electronics **42** (7) 625–633 (2012)

OPTICAL IMAGE FORMING AND PROCESSING

PACS numbers: 42.30.Va; 42.25.Kb; 42.25.Hz
DOI: 10.1070/QE2012v042n07ABEH014824

Reference-free method for forming a three-dimensional image and determining the angular velocity of a remote object

V.I. Mandrosov

Abstract. **We propose a reference-free method for forming a three-dimensional image and for determining the angular velocity of a remote nonplanar object. The method is based on probing an object by laser radiation with a coherence length that is smaller or larger than the size of the object and on the use of a screen with radial holes in the centres of which photodetectors are located, the screen being mounted in the region of the flat image of the object. A three-dimensional image of the object is constructed using the visibility of the interference fringes formed behind the screen due to radiation beams scattered by the object which pass through various pairs of holes (one of the holes is fixed). The three components of the angular velocity vector of the object are determined by the power spectrum of the electric signal produced during the movement of interference fringes on a photodetector mounted behind the screen.**

Keywords: *visibility of interference fringes, reconstruction of three-dimensional images of remote objects by their flat coherent images, Doppler effect.*

1. Introduction

Three-dimensional images of objects (or, alternatively, reconstruction of the shape of their surface by laser radiation) were first obtained in the early 1960s thanks to fundamental papers [1, 2] in the field of holography. Such images are reconstructed by a hologram formed in a photosensitive medium by superposing a reference wave from a laser source and a wave scattered by an object when it is probed by the same radiation source. The possibility of determining the velocity parameters of objects, including the angular velocity of their rotation, with the help of a probe laser beam focused on individual sections of the object, by the Doppler frequency shifts of scattered radiation (the shifts are calculated by the temporal spectrum of the sum of a reference and scattered waves) was considered in [3]. However, in the case of very remote objects, including the near-Earth space objects, the implementation of these methods requires the use of high-power laser beams with a coherence length of no less than the total distance from the source to the object and from the object to the recording medium, the beams being focused on small sections of the object surface. The sources of such radiation and systems focusing beams into separate sections of objects are very difficult to implement.

V.I. Mandrosov Moscow Institute of Physics and Technology (State University), Institutskii per. 9, 141700 Dolgoprudnyi, Moscow region, Russia; e-mail: vmandrosov@mail.ru

Received 7 February 2012; revision received 24 April 2012
Kvantovaya Elektronika **42** (7) 625–633 (2012)
Translated by I.A. Ulitkin

Later, there appeared papers devoted to reference-free methods for reconstructing a three-dimensional image of the object and determining its velocity parameters based on the use of only one laser beam probing the object. In particular, Bakut et al. [4] proposed a reference-free method for determining the angular velocity of an object's rotation that is implemented using a device containing a probe laser source, a receiving optical system forming a laser image of the object, and two holes in the plane of the image. Beams of radiation scattered by an object, passing through the holes, formed interference fringes behind the image. When rotating an object, these fringes moved to the input hole of the photodetector. The angular velocity of rotation was determined by the temporal spectrum of the electric signal produced at the photodetector output when moving the fringes. In [5] we proposed a scheme containing three such devices whose receiving optical systems formed three images of an object from three different angles. This scheme made it possible to determine the vector of the angular rotation velocity of an object. In [6, 7] we analysed the possibility of three-dimensional image reconstruction of a remote nonplanar object by the contrast of speckles of a time-averaged intensity distribution in its coherent image, based on the temporal approach, which consists in using the time correlation function of probe radiation. However, the methods proposed in [5–7] did not allow one to simultaneously reconstruct the three-dimensional image of a remote object and to determine three components of the angular velocity vector of its rotation. In this paper we report a reference-free method making it possible to reconstruct an image using a temporary approach, which is especially important in problems of determining the shape and motion parameters of near-Earth space objects.

2. Reconstruction of a three-dimensional image of an object and determination of three components of its angular velocity of rotation

2.1. Registration of planar images of an object

The laser source (*1*) (Fig. 1) probes an object (*2*) by quasi-monochromatic radiation with a time correlation envelope function

$$B_{\mathrm{u}}(\tau) = \frac{1}{T_{\mathrm{s}}}\int_{t_0}^{t_0+T_{\mathrm{s}}} u(t+\tau)u^*(t)\,\mathrm{d}t$$

and the correlation time

$$\tau_{\mathrm{c}} = \int_{-\infty}^{\infty} u^2(\tau)\,\mathrm{d}\tau,$$

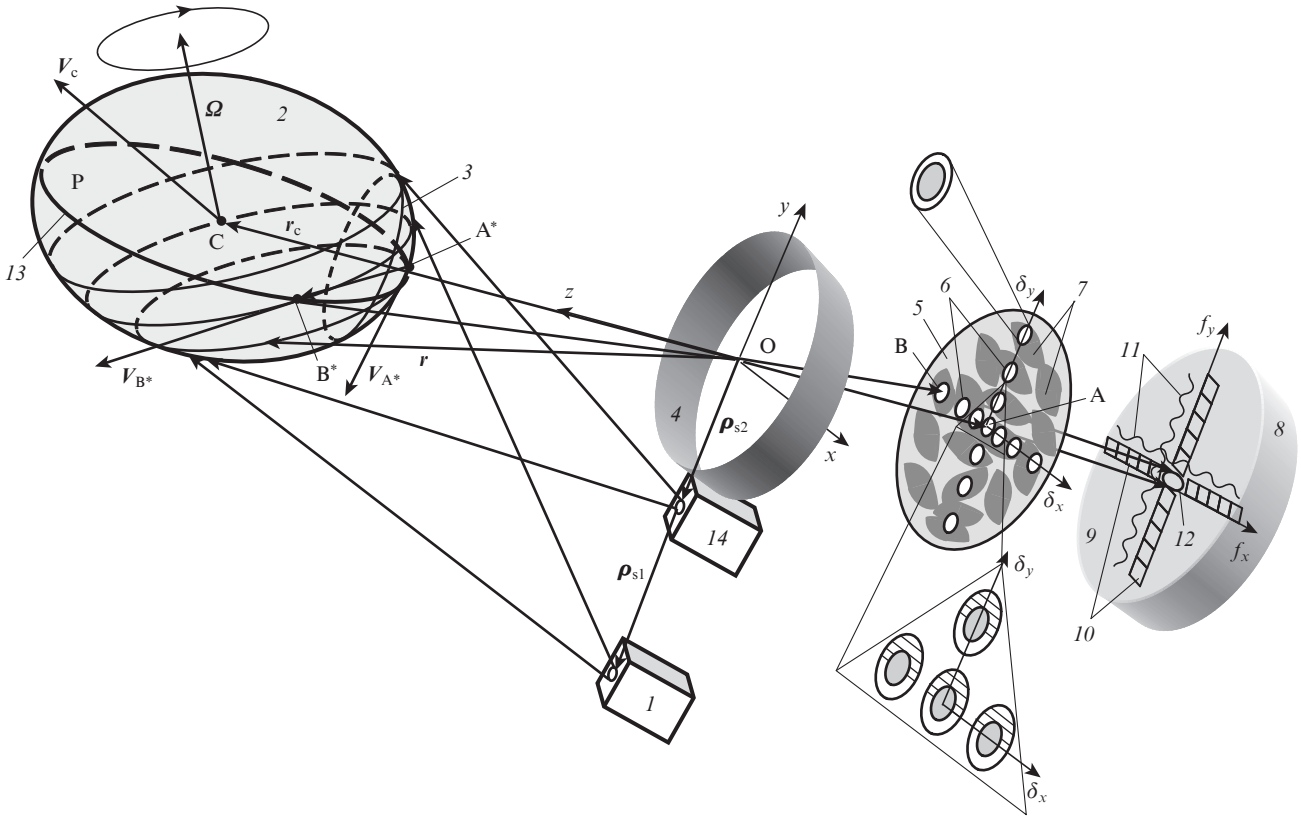

Figure 1. Scheme for simultaneous reconstruction of a three-dimensional image of an object and determination of three vector components of its angular rotation velocity:
(*1*) probe laser source; (*2*) object under study (solid body); (*3*) boundary of the region of backscattered probe radiation, which determines the visible surface of the object; (*4*) receiving optical system forming the image of the object (*2*) [the centre of the receiving aperture O is the origin of the coordinate system *zyx* with the axis *z* directed along the optical axis of the system (*4*)]; (*5*) opaque screen, which is placed in the image plane of the object (*2*); (*6*) holes in the screen (*5*) [shown are the holes located along the coordinate axes *x* and *y*, including holes, whose centres A and B have the coordinates $\delta_{x\mathrm{A}} = 0$, $\delta_{y\mathrm{A}} = 0$ and $\delta_{x\mathrm{B}} = 0$, $\delta_{y\mathrm{B}} = 0$, and points A* and B* on the surface of the object (*2*), which are optically conjugate with points A and B]; (*7*) spotted structure in the image of the object (*2*); (*8*) unit forming a three-dimensional image and determining the vector of the angular rotation velocity $\boldsymbol{\Omega}$ of the object (*2*); (*9*) plane of the receiving aperture of the unit (*8*), where photodetectors are mounted; (*10*) two mutually perpendicular linear array of photodetectors on which sinusoidal interference patterns (*11*) are projected, which are formed by radiation propagating from the object (*2*) and diffracted by the pairs of holes located on the axes *x* and *y*; (*12*) round photodetector with a centre at the origin of the coordinate system $f_x f_y$, used to determine the vector of the angular rotation velocity $\boldsymbol{\Omega}$ of the object (*2*); (*13*) cross section of the surface of the object (*2*) by the plane P, passing through points C, A*, B*, O, A, B and coordinate axes x, δ_x, f_x parallel to each, whose form is determined in the unit (*8*) by processing the interference patterns formed along the axis *x*; (*14*) additional probe laser source.

where $u(t)$ is the modulation function of the field envelope of the radiation source; t_0 and T_s are the initial time and processing time of radiation scattered by the object. Monochromatic radiation (radiation at a frequency ω_m with the coherence length substantially greater than the depth of the region of radiation backscattered by the object h_b, and the modulation function of the radiation source $u(t) \approx 1$ [8]) is used to determine the vector of angular rotation velocity of the object. Quasi-monochromatic radiation at a frequency ω_q is used to reconstruct a three-dimensional image of the object and has a coherence length $L_c = c\tau_c$ (c is the speed of light) that is smaller than the depth h_b. In accordance with the temporal approach this reconstruction will be based on the use of the function $B_u(\tau)$.

Radiation scattered by the object is focused by the optical system (*4*) on a flat opaque screen (*5*) with radially arranged holes (*6*) having diameter d_ρ, on which two flat spotted images of the object (*2*) are formed at frequencies ω_m and ω_q with an average size of spots (speckles) $a = \lambda_q d_\rho / z_{sc}$, where $\lambda_q = 2\pi c/\omega_q$, and z_{sc} is the distance from point O to the screen (*5*), i.e., to the image plane of the object. In the centre of each hole there is an integrated photodetector with a diameter d_0. At the output of the photodetector there is a narrow-band filter with peak transmission at a frequency ω_q, the hole diameter being less than $2d_0$. In Fig. 1 the photodetector in the centre of the hole is shown as a gray circle.

Let the distribution $\xi(\boldsymbol{r})$ of the heights of roughness on the surface of the object under study be specified, where $\boldsymbol{r}(x,y) = [x, y, z(x,y)]$ is the radius vector of its middle surface, and $z = z(x,y)$ is the equation of this surface. Then in the coordinate system $\delta_x \delta_y$ the instantaneous field distribution in a flat image of the object (*2*) at a frequency ω_m will have the form

$$E_{im}(t, \boldsymbol{\delta}_\perp) \sim E_0 \int k(\boldsymbol{r}) \exp[2\pi \mathrm{i} \boldsymbol{r} \boldsymbol{\rho}_{s1}/(r\lambda_m)] \times \exp\{2\pi \mathrm{i}[V_n + V_\perp(\boldsymbol{r})]t/\lambda_m\} \times \exp[2\pi \mathrm{i} q_N(\boldsymbol{r}) \xi(\boldsymbol{r})/\lambda_m] h_m(\boldsymbol{r}, \boldsymbol{\delta}_\perp) \mathrm{d}\boldsymbol{r}. \quad (1)$$

In formula (1) we introduced the following notations: E_0 is the field at the aperture of the probe radiation source; $\boldsymbol{\rho}_{s1}$ is the

radius vector of the radiation source; $\boldsymbol{\delta}_\perp = (\delta_x, \delta_y)$; $\lambda_m = 2\pi c/\omega_m$; $q_N(\boldsymbol{r}) = [q^2 - q_\perp^2(\boldsymbol{r})]^{1/2}$; $q_\perp(\boldsymbol{r}) = \boldsymbol{q}\boldsymbol{N}(\boldsymbol{r})$; $\boldsymbol{N}(\boldsymbol{r})$ is the normal to the surface of the object; $\boldsymbol{q} = (\boldsymbol{r}_c - \boldsymbol{\rho}_{s1})/|\boldsymbol{r}_c - \boldsymbol{\rho}_{s1}| + \boldsymbol{r}_c/r_c$ is the scattering vector; $\boldsymbol{r}_c$ is the radius vector of the centre of gravity of the object (*2*); $h_m(\boldsymbol{r},\boldsymbol{\delta}_\perp) = (1/S_\rho)\int\Lambda(\boldsymbol{\rho})\exp[2\pi\boldsymbol{\rho}(\boldsymbol{r}/r_c + \boldsymbol{\delta}_\perp/z_{sc})/\lambda_m]d\rho$ is the pulse response of the optical system (*4*) at a frequency ω_m; $\boldsymbol{\rho}(x,y)$ is the radius vector in the plane of the receiving aperture of the optical system (*4*); $S_\rho = \pi d_\rho^2/4$ is the area of the receiving aperture; $\Lambda(\boldsymbol{\rho})$ is the function of a pupil of the receiving optical system (*4*), forming an image of the object (*2*); $k(\boldsymbol{r})$ is the distribution of the Fresnel reflection coefficient on the surface of the image; $V_n = \boldsymbol{V}_c\boldsymbol{q}$ and $V_\perp(\boldsymbol{r}) = [\boldsymbol{\Omega}\times(\boldsymbol{r}(x,y) - \boldsymbol{r}_c)]\boldsymbol{q}$ are the tangential and radial velocity components of the object; $\boldsymbol{V}_c$ and $\boldsymbol{\Omega}$ are the velocity of the centre of gravity and the angular rotation velocity of the object. The field distribution in the instantaneous flat image of the object at a frequency ω_q is given by

$$\begin{aligned} E_{iq}(t,\boldsymbol{\delta}_\perp) \sim{}& E_0\int k(\boldsymbol{r})\exp[2\pi i\boldsymbol{r}\boldsymbol{\rho}_{s1}/(r\lambda_q)] \\ &\times u(t - 2r/c)\exp\{[2\pi i V_n + V_\perp(\boldsymbol{r})]t/\lambda_q\} \\ &\times \exp[2\pi i q_N(\boldsymbol{r})\xi(\boldsymbol{r})/\lambda_q]h_q(\boldsymbol{r},\boldsymbol{\delta}_\perp)\,d\boldsymbol{r}, \end{aligned} \tag{2}$$

where $h_q(\boldsymbol{r},\boldsymbol{\delta}_\perp) = (1/S_\rho)\int\Lambda(\boldsymbol{\rho})\exp[2\pi\boldsymbol{\rho}(\boldsymbol{r}/r_c + \boldsymbol{\delta}_\perp/z_{sc})/\lambda_q]d\boldsymbol{\rho}$ is the pulse response of the system (*4*) at a frequency ω_q.

2.2. Reconstruction of a three-dimensional image of an object

The flat image of the object at a frequency ω_q can be used below to reconstruct its three-dimensional image using two holes with centres at points A and B, which are optically conjugate to points A* and B*, located on the surface of the object (Fig. 1). The coordinates of these points are related as $x_{A*} = -\mu\delta_{xA}$, $y_{A*} = -\mu\delta_{yA}$, $x_{B*} = -\mu\delta_{xB}$, $y_{B*} = -\mu\delta_{yB}$, where $\mu = r_c/z_{sc}$ is the scale factor. In view of relations (1) and (2), provided that $\lambda_q d_\rho/z_{sc} > 5d_0$, we have

$$\begin{aligned} E_{im}(t,\boldsymbol{\delta}_{\perp A}) \sim{}& \exp(2\pi i V_n t/\lambda_m)\exp[2\pi i\boldsymbol{r}_{A*}\boldsymbol{\rho}_{s1}/(r\lambda_m)] \\ &\times \exp[2\pi i V_\perp(\boldsymbol{r}_{A*})t/\lambda_m]F_m(\boldsymbol{\delta}_{\perp A}), \\ E_{im}(t,\boldsymbol{\delta}_{\perp B}) \sim{}& \exp(2\pi i V_n t/\lambda_m)\exp[2\pi i\boldsymbol{r}_{B*}\boldsymbol{\rho}_{s1}/(r\lambda_m)] \\ &\times \exp[2\pi i V_\perp(\boldsymbol{r}_{B*})t/\lambda_m]F_m(\boldsymbol{\delta}_{\perp B}), \end{aligned} \tag{3}$$

$$\begin{aligned} E_{iq}(t,\boldsymbol{\delta}_{\perp A}) \sim{}& \exp(2\pi i V_n t/\lambda_q)\exp[2\pi i\boldsymbol{r}_{A*}\boldsymbol{\rho}_{s1}/(r\lambda_q)] \\ &\times u(t - 2r_{A*}/c)\exp[2\pi i V_\perp(\boldsymbol{r}_{A*})t/\lambda_q]F_q(\boldsymbol{\delta}_{\perp A}), \\ E_{iq}(t,\boldsymbol{\delta}_{\perp B}) \sim{}& \exp(2\pi i V_n t/\lambda_q)\exp[2\pi i\boldsymbol{r}_{B*}\boldsymbol{\rho}_{s1}/(r\lambda_q)] \\ &\times u(t - 2r_{B*}/c)\exp[2\pi i V_\perp(\boldsymbol{r}_{B*})t/\lambda_q]F_q(\boldsymbol{\delta}_{\perp B}), \end{aligned} \tag{4}$$

where

$$\begin{aligned} F_q(\boldsymbol{\delta}_\perp) = F_q(x = -\mu\delta_x, y = -\mu\delta_y) = {}& \iint k(x,y)h_q(x + \mu\delta_x, y + \mu\delta_y) \\ &\times \exp[2\pi i q_N\xi(x,y)/\lambda_q]\,dx\,dy; \\ F_m(\boldsymbol{\delta}_\perp) = F_m(x = -\mu\delta_x, y = -\mu\delta_y) = {}& \iint k(x,y)h_m(x + \mu\delta_x, y + \mu\delta_y) \\ &\times \exp[2\pi i q_N\xi(x,y)/\lambda_m]\,dx\,dy; \end{aligned} \tag{5}$$

$\boldsymbol{\delta}_{\perp A} = (\delta_{xA}, \delta_{yA})$; $\boldsymbol{\delta}_{\perp B} = (\delta_{xB}, \delta_{yB})$. At the time of registration $T_s \gg \tau_c$, and provided that $\lambda_q d_\rho/z_{sc} > 5d_0$, the photodetectors in the holes with centres at points A and B register time-averaged intensities T_s

$$\begin{aligned} \bar{I}_q(\boldsymbol{\delta}_{\perp A}) = \frac{1}{T_s}\int_{t_0}^{t_0+T_s}|E_{iq}(t,\boldsymbol{\delta}_{\perp A})|^2 dt \sim |F_q(\boldsymbol{\delta}_{\perp A})|^2, \\ \bar{I}_q(\boldsymbol{\delta}_{\perp B}) = \frac{1}{T_s}\int_{t_0}^{t_0+T_s}|E_{iq}(t,\boldsymbol{\delta}_{\perp B})|^2 dt \sim |F_q(\boldsymbol{\delta}_{\perp B})|^2. \end{aligned} \tag{6}$$

As follows from [5, 6], at a sufficiently high resolution of the system (*4*) we have $|F_q(\boldsymbol{\delta}_\perp)|^2 \approx \langle|F_q(\boldsymbol{\delta}_\perp)|^2\rangle_\xi \sim k_{iq}(\boldsymbol{\delta}_\perp) = k_{iq}(x = -\mu\delta_x, y = -\mu\delta_y)$, where the angle brackets $\langle\ldots\rangle_\xi$ denote averaging over the distribution of heights of the surface roughness $\xi(x,y)$ of the object (*2*):

$$\begin{aligned} k_{iq}(x = -\mu\delta_x, y = -\mu\delta_y) \approx{}& (\ell_\xi/\sigma_\xi)^2|k(x = -\mu\delta_x, y = -\mu\delta_y)|^2 \\ &\times \exp[-\tan^2\vartheta(\ell_\xi/\sigma_\xi)^2]; \end{aligned} \tag{7}$$

$\vartheta = \arctan(q_\perp/q_N)$ is the angle between the normal $\boldsymbol{N}$ to the surface of the object and the scattering vector $\boldsymbol{q}$; σ_ξ and ℓ_ξ are the root-mean-square deviation (rms deviation) and the correlation radius of the distribution $\xi(\boldsymbol{r})$. According to [4, 5] the function $k_{iq}(x = -\mu\delta_x, y = -\mu\delta_y)$ is proportional to the intensity distribution $\bar{I}_q(\boldsymbol{\delta}_\perp)$ in the optical image of the object and the brightness $L(x = -\mu\delta_x, y = -\mu\delta_y)$ of small areas of the object surface optically conjugate to small areas of its flat image on the screen (*5*). Therefore, in view of (6) and (7) we have

$$\begin{aligned} L(\boldsymbol{r}_{A*}) \sim \bar{I}_q(\boldsymbol{\delta}_{\perp A}) \sim |F_q(\boldsymbol{\delta}_{\perp A})|^2 \sim k_{iq}(x_{A*}, y_{A*}), \\ L(\boldsymbol{r}_{B*}) \sim \bar{I}_q(\boldsymbol{\delta}_{\perp B}) \sim |F_q(\boldsymbol{\delta}_{\perp B})|^2 \sim k_{iq}(x_{B*}, y_{B*}), \end{aligned} \tag{8}$$

where $L(\boldsymbol{r}_{A*})$ and $L(\boldsymbol{r}_{B*})$ are sites of the surface brightness in a small neighbourhood of points A* and B*. Knowing the function $\bar{I}_q(\boldsymbol{\delta}_{\perp B})$, provided that $\boldsymbol{\delta}_{\perp A} = (0,0)$, we can determine the depth h_b and width d_b of the backscattering region (Fig. 1). For example, if the object under study has a spherical form, with a constant coefficient $|k|^2$, we obtain $\bar{I}_q(\boldsymbol{\delta}_{\perp B}) \sim \bar{I}_q(0,0)\times\exp[-(\delta_{\perp B}/\rho_0)^2(\ell_\xi/\sigma_\xi)^2]$ [5]. Defining below the boundary of the backscattering region $\delta_{\perp B} = \delta_{\perp b}$, so that the relation $\bar{I}_q(\boldsymbol{\delta}_{\perp b}) \sim \bar{I}_q(0,0)\exp(-2)$ held true, we obtain $\delta_{\perp b} \approx \rho_0[\sigma_\xi/(2\ell_\xi)]$, $h_b \approx \rho_0[\sigma_\xi/(2\ell_\xi)]^2$ and $d_b = 2\delta_{\perp b} \approx \rho_0(\sigma_\xi/\ell_\xi)$, where ρ_0 is the radius of curvature of the surface of the object.

Waves propagating from the two holes form sinusoidal interference fringes on the receiving aperture (*9*) of the unit (*8*). We choose a coordinate system $f_x f_y f_z$ with the axis f_z, directed along the optical axis of the system (*4*), with the coordinate plane $f_x f_y$, coincident with the plane of the receiving aperture (*9*), and the axis f_x directed along these fringes. In this system, taking into account relation (4), provided that the $T_s \ll \lambda_q/(\Omega d_b)$, the intensity distribution in the interference fringes has the form

$$\begin{aligned} I_q(t,\boldsymbol{f}) = |E_q(t,\boldsymbol{f})|^2 \sim{}& |F_q(\boldsymbol{\delta}_{\perp A})|^2 + |F_q(\boldsymbol{\delta}_{\perp B})|^2 \\ &+ H(t,\boldsymbol{f}) + H^*(t,\boldsymbol{f}), \end{aligned}$$

where

$$\begin{aligned} E_q(t,\boldsymbol{f}) \sim{}& E_{iq}(t,\boldsymbol{\delta}_{\perp A})\exp[2\pi i\boldsymbol{\delta}_A\boldsymbol{f}/(z_f\lambda_q)] \\ &+ E_{iq}(t,\boldsymbol{\delta}_{\perp B})\exp[2\pi i\boldsymbol{\delta}_B\boldsymbol{f}/(z_f\lambda_q)] \end{aligned}$$

is the field distribution in these fringes;

$$H(t,\boldsymbol{f}) \approx \exp\{2\pi\mathrm{i}[(\boldsymbol{r}_{\mathrm{B}^*}-\boldsymbol{r}_{\mathrm{A}^*})\boldsymbol{\rho}_{\mathrm{s1}}/r_{\mathrm{c}} + (\boldsymbol{\delta}_{\perp\mathrm{B}}-\boldsymbol{\delta}_{\perp\mathrm{A}})\boldsymbol{f}/z_f]/\lambda_{\mathrm{q}}\}$$
$$\times u(t-2r_{\mathrm{A}^*}/c)\,u^*(t-2r_{\mathrm{B}^*}/c)\,F_{\mathrm{q}}(\boldsymbol{\delta}_{\perp\mathrm{A}})F_{\mathrm{q}}^*(\boldsymbol{\delta}_{\perp\mathrm{B}});$$

z_f is the distance from the screen (*5*) to the plane of the receiving aperture (*9*). The distribution $I_{\mathrm{q}}(t,\boldsymbol{f})$ is recorded along the axis f_x by a linear array of photodetectors (*10*), at the outputs of which narrow-band filters with maximum transmission at a frequency ω_{q} are mounted. Then, the unit (*8*) calculates the time-averaged ($T_{\mathrm{s}} \gg \tau_{\mathrm{c}}$) intensity distribution in the interference fringes

$$\bar{I}_{\mathrm{q}}(\boldsymbol{f}) = \frac{1}{T_{\mathrm{s}}}\int_{t_0}^{t_0+T_{\mathrm{s}}} I_{\mathrm{q}}(t,\boldsymbol{f})\,\mathrm{d}t.$$

Taking into account relation (8)

$$\bar{I}_{\mathrm{q}}(\boldsymbol{f}) \sim \bar{I}_{\mathrm{q}}(\boldsymbol{\delta}_{\perp\mathrm{A}}) + \bar{I}_{\mathrm{q}}(\boldsymbol{\delta}_{\perp\mathrm{B}}) + 2B_u[2(r_{\mathrm{A}^*}-r_{\mathrm{B}^*})/L_{\mathrm{c}}]$$
$$\times\cos[2\pi(\boldsymbol{\delta}_{\perp\mathrm{B}}-\boldsymbol{\delta}_{\perp\mathrm{A}})\boldsymbol{f}/(z_f\lambda_{\mathrm{q}}) + \psi_{\mathrm{ABq}}]$$
$$\times\,|\bar{I}_{\mathrm{iq}}(\boldsymbol{\delta}_{\perp\mathrm{A}})\,\bar{I}_{\mathrm{iq}}(\boldsymbol{\delta}_{\perp\mathrm{B}})|^{1/2}, \qquad (9)$$

where

$$B_u[2(r_{\mathrm{A}^*}-r_{\mathrm{B}^*})/L_{\mathrm{c}}] = \frac{1}{T_{\mathrm{s}}}\int_{t_0}^{t_0+T_{\mathrm{s}}} u(t-2r_{\mathrm{A}^*}/c)\,u^*(t-2r_{\mathrm{B}^*}/c)\mathrm{d}t;$$

$$\psi_{\mathrm{ABq}} = 2\pi(\boldsymbol{r}_{\mathrm{A}^*}-\boldsymbol{r}_{\mathrm{B}^*})\boldsymbol{\rho}_{\mathrm{s1}}/(r\lambda_{\mathrm{q}})$$
$$+\arctan\{\mathrm{Re}[F_{\mathrm{q}}(\boldsymbol{\delta}_{\perp\mathrm{A}})F_{\mathrm{q}}^*(\boldsymbol{\delta}_{\perp\mathrm{B}})]/\mathrm{Im}[F_{\mathrm{q}}(\boldsymbol{\delta}_{\perp\mathrm{A}})F_{\mathrm{q}}^*(\boldsymbol{\delta}_{\perp\mathrm{B}})]\}.$$

For a remote object $B_u[2(r_{\mathrm{A}^*}-r_{\mathrm{B}^*})/L_{\mathrm{c}}] \approx B_u(2Z_{\mathrm{A}^*\mathrm{B}^*}/L_{\mathrm{c}})$, where $Z_{\mathrm{A}^*\mathrm{B}^*} = Z(x_{\mathrm{A}^*},y_{\mathrm{A}^*},x_{\mathrm{B}^*},y_{\mathrm{B}^*}) \approx r_{\mathrm{A}^*}-r_{\mathrm{B}^*}$ is the difference in the distance from the receiving aperture of the system (*4*) to points A^* and B^*. The main characteristic of the interference fringes is their visibility [9]

$$V_{\mathrm{q}}(Z_{\mathrm{A}^*\mathrm{B}^*}) = [\bar{I}_{\mathrm{q}}(\boldsymbol{f}_{\max}) - \bar{I}_{\mathrm{q}}(\boldsymbol{f}_{\min})]/[\bar{I}_{\mathrm{q}}(\boldsymbol{f}_{\max}) + \bar{I}_{\mathrm{q}}(\boldsymbol{f}_{\min})]$$
$$= |B_u(2Z_{\mathrm{A}^*\mathrm{B}^*}/L_{\mathrm{c}})|\,V_{\mathrm{AB}},$$

where, taking into account relations (6)–(9)

$$V_{\mathrm{AB}} = 2|F_{\mathrm{q}}(\boldsymbol{\delta}_{\perp\mathrm{A}})F_{\mathrm{q}}(\boldsymbol{\delta}_{\perp\mathrm{B}})|/[|F_{\mathrm{q}}(\boldsymbol{\delta}_{\perp\mathrm{A}})|^2 + |F_{\mathrm{q}}(\boldsymbol{\delta}_{\perp\mathrm{B}})|^2]$$
$$= 2|\bar{I}_{\mathrm{iq}}(\boldsymbol{\delta}_{\perp\mathrm{A}})\bar{I}_{\mathrm{iq}}(\boldsymbol{\delta}_{\perp\mathrm{B}})|^{1/2}/[\bar{I}_{\mathrm{iq}}(\boldsymbol{\delta}_{\perp\mathrm{A}}) + \bar{I}_{\mathrm{iq}}(\boldsymbol{\delta}_{\perp\mathrm{B}})]. \qquad (10)$$

With the growth of $Z_{\mathrm{A}^*\mathrm{B}^*}$ the visibility V_{q} decreases significantly. When $Z_{\mathrm{A}^*\mathrm{B}^*} \gg L_{\mathrm{c}}$, it is virtually zero. Let the receiving optical system (*4*) 'accompany' the object (*2*) such that its optical axis passed through the object's centre of gravity and centre of gravity of its image A and intersected the surface of the object (*2*) at point A^*, nearest to the system (*4*). In this case, $\delta_{\perp\mathrm{A}} = \delta_{x\mathrm{A}} = \delta_{y\mathrm{A}} = 0$. Then in the coordinate system xyz, point A^* has the coordinates $0,0,z_{\mathrm{A}^*}$, and point B^* – the coordinates $x_{\mathrm{B}^*} = -\mu\delta_{x\mathrm{B}}$, $y_{\mathrm{B}^*} = -\mu\delta_{y\mathrm{B}}$, $z = z_{\mathrm{A}^*} + Z_{\mathrm{A}^*\mathrm{B}^*}$, where $Z_{\mathrm{A}^*\mathrm{B}^*}$ is the height of the object surface at point B^* above the plane passing through point A^*, parallel to the plane xy. These relations imply that

$$Z_{\mathrm{A}^*\mathrm{B}^*} = (L_{\mathrm{c}}/2)|B_u(\chi)|^{-1}, \qquad (11)$$

where $\chi = V_{\mathrm{q}}/V_{\mathrm{AB}} = |B_u(2Z_{\mathrm{A}^*\mathrm{B}^*}/L_{\mathrm{c}})|$. Placing the hole with the centre at point B in different parts of the screen (*5*) and recording the intensities $\bar{I}_{\mathrm{iq}}(\boldsymbol{\delta}_{\perp\mathrm{A}})$ and $\bar{I}_{\mathrm{iq}}(\boldsymbol{\delta}_{\perp\mathrm{B}})$ by the photodetectors arranged in the holes with centres at points A and B, we can use relations (8), (10) and (11) to determine the distribution of heights $Z(x_{\mathrm{B}^*},y_{\mathrm{B}^*})$ of the surface of the object under study, i.e., its shape and brightness distribution on the surface $Z(x_{\mathrm{B}^*},y_{\mathrm{B}^*}) \sim \bar{I}_{\mathrm{iq}}^2(\boldsymbol{\delta}_{\perp\mathrm{B}})$. In Appendix 1 we present another algorithm that allows simultaneous determination of the height of the surface, $Z_{\mathrm{A}^*\mathrm{B}^*}$ at point B^* and brightness $L(\boldsymbol{r}_{\mathrm{A}^*}) = L(x_{\mathrm{A}^*},y_{\mathrm{A}^*})$ and $L(\boldsymbol{r}_{\mathrm{B}^*}) = L(x_{\mathrm{B}^*},y_{\mathrm{B}^*})$ in the small neighbourhood of points A^* and B^*. In Appendix 2 we estimated the accuracy of determining the surface height $Z_{\mathrm{A}^*\mathrm{B}^*}$ in the presence of additive noise.

2.3. Determination of the angular velocity vector Ω of the object

Two holes with centres at points A and B can be used to determine the angular velocity vector $\boldsymbol{\Omega}$ of the object under study. To do this, we mounted a narrow-band filter with maximum transmission at a frequency ω_{m} at the input of the photodetector (*12*), which is located in the centre of the receiving aperture (*9*) of the unit (*8*). In this case, the photodetector (*12*) detects the time signal $I_{\mathrm{m}}(t) = |E_{\mathrm{m}}(t)|^2$, where $E_{\mathrm{m}}(t) = E_{\mathrm{im}}(t,\boldsymbol{\delta}_{\perp\mathrm{A}}) + E_{\mathrm{im}}(t,\boldsymbol{\delta}_{\perp\mathrm{B}})$. In view of relations (1) and (3),

$$I_{\mathrm{m}}(t) \sim |F_{\mathrm{m}}(\boldsymbol{\delta}_{\perp\mathrm{A}})|^2 + |F_{\mathrm{m}}(\boldsymbol{\delta}_{\perp\mathrm{B}})|^2 + H_{\mathrm{m}}(t) + H_{\mathrm{m}}^*(t), \qquad (12)$$

where

$$H_{\mathrm{m}}(t) = \exp\{2\pi\mathrm{i}[\boldsymbol{\Omega}\times(\boldsymbol{r}_{\mathrm{A}^*}-\boldsymbol{r}_{\mathrm{B}^*})]\boldsymbol{q}t/\lambda_{\mathrm{m}} + \mathrm{i}\gamma_{\mathrm{m}}\}$$
$$\times F_{\mathrm{m}}(\boldsymbol{\delta}_{\perp\mathrm{A}})F_{\mathrm{m}}^*(\boldsymbol{\delta}_{\perp\mathrm{B}});\quad \gamma_{\mathrm{m}} = 2\pi(\boldsymbol{r}_{\mathrm{A}^*}-\boldsymbol{r}_{\mathrm{B}^*})\boldsymbol{\rho}_{\mathrm{s1}}/(r_{\mathrm{c}}\lambda_{\mathrm{m}}).$$

Then, the unit (*8*) determines the spectrum of the signal $I_{\mathrm{m}}(t)$

$$S(\nu) \sim \frac{1}{T_{\mathrm{d}}}\int_{t_0}^{t_0+T_{\mathrm{d}}} \exp(2\pi\mathrm{i}\nu t)\,\mathrm{d}t,$$

where ν is the frequency; T_{d} is the time of the spectrum formation, chosen from the condition $\lambda_{\mathrm{m}}/(\Omega d_{\mathrm{b}}) \ll T_{\mathrm{d}} \ll d_\rho d_{\mathrm{b}}/(\Omega r_{\mathrm{c}})$. When $\lambda_{\mathrm{m}}/(\Omega d_{\mathrm{b}}) \ll T_{\mathrm{d}}$, movement of the interference fringes formed in the plane (*9*) becomes noticeable due to the interference of waves propagating from two holes with centres at points A and B with respect to the photodetector (*12*). This movement is due to the difference $\Delta\nu = \nu_{\mathrm{B}^*} - \nu_{\mathrm{A}^*}$ in the Doppler frequency shifts of radiation $\nu_{\mathrm{B}^*} = V_{\perp\mathrm{B}^*}(\boldsymbol{r})/\lambda_{\mathrm{m}}$ and $\nu_{\mathrm{A}^*} = V_{\perp\mathrm{A}^*}(\boldsymbol{r})/\lambda_{\mathrm{m}}$, scattered from small areas of the surface of a rotating object in the vicinity of points A^* и B^* (Fig. 1), where $V_{\perp\mathrm{A}^*}(\boldsymbol{r}) = V_{\mathrm{A}^*}\boldsymbol{q}$ and $V_{\perp\mathrm{B}^*}(\boldsymbol{r}) = V_{\mathrm{B}^*}\boldsymbol{q}$ are the projections of the velocity vectors $\boldsymbol{V}_{\mathrm{A}^*} = \boldsymbol{\Omega}\times[\boldsymbol{r}_{\mathrm{A}^*}(x,y) - \boldsymbol{r}_{\mathrm{c}}]$ and $\boldsymbol{V}_{\mathrm{B}^*} = \boldsymbol{\Omega}\times[\boldsymbol{r}_{\mathrm{B}^*}(x,y) - \boldsymbol{r}_{\mathrm{c}}]$ of revolution of these points around the axis of rotation of the object on the scattering vector $\boldsymbol{q}$.

The function $S(\nu)$ has a central peak (zero order) at a frequency $\nu_0 = 0$ and two side maxima (±1st orders) at frequencies $\nu_\pm = \pm(\boldsymbol{\Omega}\times\boldsymbol{d}\boldsymbol{q})/\lambda_{\mathrm{m}}$, where, taking into account the fact that $\delta_{x\mathrm{A}} = \delta_{y\mathrm{A}} = 0$, $\boldsymbol{d} = \boldsymbol{r}_{\mathrm{A}^*}(x,y) - \boldsymbol{r}_{\mathrm{B}^*}(x,y)$ is a vector with the components

$$d_x = -\mu\delta_{x\mathrm{B}},\ d_y = -\mu\delta_{y\mathrm{B}},\ d_z = z_{\mathrm{B}^*} - z_{\mathrm{A}^*} = Z_{\mathrm{A}^*\mathrm{B}^*}. \qquad (13)$$

In what follows we shall deal only with that part of the spectrum $S(\nu)$, which is in the range $\nu \leqslant 3/T_{\mathrm{d}} < \infty$. This part contains the +1st order at the frequency ν_+. Taking into account relations (12) and $\delta_{x\mathrm{A}} = \delta_{y\mathrm{A}} = 0$ this part of the spectrum can be represented as

$$S(\nu) \approx \frac{1}{T_\mathrm{d}}\int_{t_0}^{t_0+T_\mathrm{d}} \exp(2\pi \mathrm{i}\nu t)\,\mathrm{d}t$$

$$= \mathrm{sinc}[T_\mathrm{d}(-\nu_+ + \nu)]\exp(\mathrm{i}\gamma_\mathrm{m})F_\mathrm{m}(\boldsymbol{\delta}_{\perp\mathrm{A}}=0)F_\mathrm{m}^*(\boldsymbol{\delta}_{\perp\mathrm{B}}). \quad (14)$$

We also assume that the source of the probe radiation is mounted so that the condition $\boldsymbol{\rho}_{\mathrm{s}1}/r_\mathrm{c} \ll 1$ is fulfilled. Then, for the scattering vector $\boldsymbol{q}$ we have the relation $\boldsymbol{q} \approx 2\boldsymbol{k} - 2\boldsymbol{\rho}_{\mathrm{s}1}/r_\mathrm{c}$, where $\boldsymbol{k}$ is the unit vector directed along the axis z. If the components of the radius vector $\rho_{\mathrm{s}1x}$ and $\rho_{\mathrm{s}1z}$ are equal to zero (Fig. 1), taking into account relations (13) and

$$\boldsymbol{\Omega}\times\boldsymbol{d} = \boldsymbol{i}(\Omega_y d_z - \Omega_z d_y) + \boldsymbol{j}(\Omega_z d_x - \Omega_x d_z) + \boldsymbol{k}(\Omega_x d_y - \Omega_y d_x),$$

where $\boldsymbol{i}$ and $\boldsymbol{j}$ are the unit vectors directed along the axes δ_x and δ_y, we obtain

$$\nu_+ = 2\{\mu(\Omega_y\delta_{x\mathrm{B}} - \Omega_x\delta_{y\mathrm{B}})$$

$$+ \rho_{\mathrm{s}1y}[\mu\Omega_z\delta_{x\mathrm{B}} + \Omega_x Z_{\mathrm{A}^*\mathrm{B}^*}]/r_\mathrm{c}\}/\lambda_\mathrm{m}. \quad (15)$$

Then, changing the position of the centre of the hole at point B and the source of probe radiation, and using relation (15), we can derive three equations which determine three components of the angular velocity vector $\boldsymbol{\Omega}$ of the object (*2*) (Fig. 1).

Let us now analyse the effect of additive temporal noise on the accuracy of determining the velocity $\boldsymbol{\Omega}$, which is used by the photodetector (*12*) to detect the signal $I_{\mathrm{m}\Sigma}(t) \approx |E_\mathrm{m}(t) + E_\mathrm{n}(t)|^2$, where $E_\mathrm{n}(t)$ is the noise field. The correlation function of the field $\langle E_\mathrm{n}(t_1)E_\mathrm{n}^*(t_2)\rangle_\mathrm{n} = \sigma_\mathrm{n}^2 w(t_1 - t_2)$, where the angle brackets $\langle\ldots\rangle_\mathrm{n}$ denote averaging over different realisations of the noise field, and $\sigma_\mathrm{n} = \langle|E_\mathrm{n}(t_0)|^2\rangle_\mathrm{n}^{1/2}$ and $w(t_1 - t_2)$ are its rms deviation and correlation coefficient. Without loss of generality, we restrict ourselves to the case of rotation of an object about an axis parallel to the y axis ($\Omega_z = 0$, $\Omega_x = 0$). In the absence of noise, when $E_\mathrm{n}(t) = 0$, from (15) we obtain the angular velocity of the object $\Omega_y = \nu_+/(2\mu\delta_{x\mathrm{B}})$. In the presence of noise and the condition $I_\mathrm{m}(t) \gg |E_\mathrm{n}(t)|^2$ the spectrum of the signal received by the photodetector (*12*) is given by

$$\hat{S}(\nu) \sim \frac{1}{T_\mathrm{d}}\int_{t_0}^{t_0+T_\mathrm{d}} I_{\mathrm{m}\Sigma}(t)\exp(2\pi\mathrm{i}\nu t)\,\mathrm{d}t = S(\nu) + \Delta S(\nu),$$

where

$$\Delta S(\nu) = \frac{1}{T_\mathrm{d}}\int_{t_0}^{t_0+T_\mathrm{d}} [E_\mathrm{m}(t)E_\mathrm{n}^*(t) + E_\mathrm{m}^*(t)E_\mathrm{n}(t)]\exp(2\pi\mathrm{i}\nu t)\,\mathrm{d}t.$$

The angular velocity Ω_y in the presence of noise will be estimated using the expression $\tilde{\Omega}_y = \tilde{\nu}_+/(2\mu\delta_{x\mathrm{B}})$, where

$$\tilde{\nu}_+ = \int_{3/T_\mathrm{d}}^{2\nu_{+\mathrm{b}}} \nu\tilde{S}(\nu)\,\mathrm{d}\nu \Big/ \int_{3/T_\mathrm{d}}^{2\nu_{+\mathrm{b}}} \tilde{S}(\nu)\,\mathrm{d}\nu$$

is the evaluation of the frequency parameter ν_+; $\nu_{+\mathrm{b}} = \Omega_{y\mathrm{b}}/(2\mu\delta_{x\mathrm{B}})$ is the upper limit of integration; $\Omega_{y\mathrm{b}}$ is the largest predicted angular velocity of the object. Under the assumption that $\langle E_\mathrm{n}(t)\rangle_\mathrm{n} = 0$, estimation of $\tilde{\Omega}_y$ is not biased. This means that $\langle\tilde{\nu}_+\rangle_\mathrm{n} = \nu_+$ and $\langle\tilde{\Omega}_y\rangle_\mathrm{n} = \Omega_y$. The relative accuracy of estimating the angular velocity $\tilde{\Omega}_y$ is given by the expression $\eta_\Omega = |\langle(\Delta\Omega_y)^2\rangle_\mathrm{n}^{1/2}|/\Omega_y = \langle(\Delta\nu_+)^2\rangle_\mathrm{n}/\nu_+$ ($\Delta\Omega_y = \tilde{\Omega}_y - \Omega_y$, $\Delta\nu_+ = \tilde{\nu}_+ - \nu_+$) using the relation $\langle\tilde{\nu}_+\rangle_\mathrm{n} = \nu_+\langle(\Delta\nu_+)^2\rangle_\mathrm{n} \approx \langle(\int\nu\Delta S(\nu)\mathrm{d}\nu)^2\rangle_\mathrm{n}/[\int S(\nu)\mathrm{d}\nu]^2$.

Taking into account this relation, as well as formulas (3) and (14) under the conditions $\nu_+ T_\mathrm{d} \gg 1$ and $T_\mathrm{d} \gg \tau_\mathrm{n}$ we have

$$\eta_\Omega \approx \nu_{+\mathrm{b}}\sigma_\mathrm{n}\{\tau_\mathrm{n}\nu_{+\mathrm{b}}/[\bar{I}_\mathrm{m}(\boldsymbol{\delta}_{\perp\mathrm{A}}=0)\,\bar{I}_\mathrm{m}(\boldsymbol{\delta}_{\perp\mathrm{B}})]^{1/2}\}^{1/2}/\nu_+,$$

where

$$\tau_\mathrm{n} = \int_{-\infty}^{+\infty} w(\tau)\mathrm{d}\tau$$

is the correlation time of the noise field;

$$\bar{I}_\mathrm{m}(0,0) = \frac{1}{T_\mathrm{d}}\int_{t_0}^{t_0+T_\mathrm{d}} |E_\mathrm{im}(t,0,0)|^2\,\mathrm{d}t \sim |F_\mathrm{m}(\boldsymbol{\delta}_{\perp\mathrm{A}}=0)|^2,$$

$$\bar{I}_\mathrm{m}(\boldsymbol{\delta}_{\perp\mathrm{B}}) = \frac{1}{T_\mathrm{d}}\int_{t_0}^{t_0+T_\mathrm{d}} |E_\mathrm{im}(t,\boldsymbol{\delta}_{\perp\mathrm{B}})|^2\,\mathrm{d}t \sim |F_\mathrm{m}^*(\boldsymbol{\delta}_{\perp\mathrm{B}})|^2$$

are the time-averaged intensities of the image of the object at points A and B at a frequency ω_m. If the holes with centres at points A and B are close, then $\bar{I}_\mathrm{m}(\boldsymbol{\delta}_{\perp\mathrm{B}}) \approx \bar{I}_\mathrm{m}(0,0)$ and

$$\eta_\Omega \approx \nu_{+\mathrm{b}}\eta_\mathrm{n}(\tau_\mathrm{n}\nu_{+\mathrm{b}})^{1/2}/\nu_+, \quad (16)$$

where $\eta_\mathrm{n} = \sigma_\mathrm{n}/\bar{I}_\mathrm{m}^{1/2}(0,0)$ is the signal-to-noise ratio.

The scheme (presented in Sections 2.2 and 2.3) allowing formation of a three-dimensional image of an object and determination of its angular velocity vector $\boldsymbol{\Omega}$ by the interference pattern formed by radiation transmitted through two holes in the screen (*5*) requires multiple repositioning of one of them for the time during which the speckle structure would not change in the image of the object. However, even with poor quality of the images of the object, consisting of thousands of speckles, about 10^3 different positions of the hole are required, because each speckle field region must match at least one position of the hole. But this structure is virtually unchanged only when you turn an object by the angle (in radians) $0.2d_\rho/r_\mathrm{c}$ [4], and for each change of position of the holes it takes (in seconds) $0.2d_\rho/(10^3\Omega r_\mathrm{c})$. However, even at slow rotation of the object with angular velocity $\Omega = 10^{-2}$ rad s^{-1} for sufficiently remote objects for which $d_\rho/r_\mathrm{c} < 10^{-3}$ it will take about 10 μs. Therefore, the proposed scheme is difficult to implement. Below, we present a scheme that makes it possible, based on the results of Sections 2.2 and 2.3, to reconstruct a three-dimensional image of the object and to determine three vector components of its angular rotation velocity.

2.4. Scheme of simultaneous reconstruction of a three-dimensional image of the object and determination of three vector components of its angular rotation velocity

Consider the scheme allowing simultaneous reconstruction of a three-dimensional image of the object and determination three vector components (Ω_x, Ω_y and Ω_z) of its angular rotation velocity $\boldsymbol{\Omega}$ (see Fig. 1).

The object (*2*) in question is probed by quasi-monochromatic radiation at $2K + 1$ frequencies $\omega_{0\mathrm{q}}$, $\omega_{-j\mathrm{q}}$ and $\omega_{j\mathrm{q}}$ ($j = 0, \ldots, K-1$) and by monochromatic radiation at a frequency $\omega_{3\mathrm{m}}$, generated by the laser source (*1*). In addition, the object is probed by monochromatic radiation at frequencies $\omega_{0\mathrm{m}}$, $\omega_{1\mathrm{m}}$ and $\omega_{2\mathrm{m}}$, generated by the additional laser source (*14*), whose radius vector of location $\rho_{\mathrm{s}2}$ has components $\rho_{\mathrm{s}2x} = \rho_{\mathrm{s}2z} = 0$, $\rho_{\mathrm{s}2y} \approx d_\rho/2$. Radiation scattered by the object is directed by the optical system (*4*) to the holes placed along different diameters of the screen (*5*). In the plane of the speckle image of the object (*7*), the screen is mounted centrally symmetric with respect to the centre of the hole at point A, whose coor-

dinates are $\delta_{x\mathrm{A}} = 0$ and $\delta_{y\mathrm{A}} = 0$. The distance between the centres of adjacent holes is $a = \lambda_{0\mathrm{q}} d_\rho / z_{\mathrm{sc}}$, where $\lambda_{0\mathrm{q}} = 2\pi c/\omega_{0\mathrm{q}}$. Radiation passed through the holes enters the unit (*8*), which forms a three-dimensional image and determines the vector of the angular rotation velocity $\boldsymbol{\Omega}$ of the object (*2*). In the centre of each hole a photodetector with diameter d_0 is placed. The holes have the same diameter equal to $\sqrt{2}d_0$, except for four holes with centres at points $(0,0)$, $(a,0)$ $(0,a)$ and $(-a,0)$, the diameter of which is $\sqrt{3}d_0$. In the screen (*5*) these four holes are shown by a triangle. Two pairs of holes with centres at points $(0,0)$, $(a,0)$ and $(0,0)$, $(0,a)$ and the source (*14*) are used to determine the components Ω_x and Ω_y, and a pair of holes with centres at points $(0,0)$ and $(-a,0)$ and the source (*1*) are used to determine the component Ω_z. Assuming that at the boundary of the screen (*5*) the distances between adjacent holes are also equal to a, we obtain that the number of different diameters is $K \approx \pi d_{\mathrm{sc}}/(2a)$, where d_{sc} is the screen size, and the angle (in radians) between the adjacent diameters is $\pi/K = 2a/d_{\mathrm{sc}}$. The coordinate system $\delta_x\delta_y$ divides the screen (*5*) into four major sectors, each of which is divided into $K/2$ smaller sectors.

We label by the letter j ($j = 0, 1, 2, ..., K-1$) all diameters ranging from the diameter coincident with the axis δ_x, whose number is $j = 0$. Then, for example, the diameter, which coincides with the axis δ_y, has the number $j = K/2$. In the polar coordinate system the centres of the holes on the right of the axis δ_x are located at points $(\rho_n, \varphi_j = \pi j/K)$, and on the left of the axis δ_x – at points $(\rho_n, \varphi_j = \pi j/K + \pi)$, where $n = 1, 2, 3, ..., N$ is the hole number; N is the total number of holes on the left and right of the axis δ_x; $\rho_n = na$. In the holes located along the jth diameter on the right of the axis δ_x, we place a narrow-band filter with maximum transmission at a frequency $\omega_{j\mathrm{q}}$, and on the left of this axis we place a narrow-band filter with maximum transmission at a frequency $\omega_{-j\mathrm{q}}$. In the shaded parts of the holes with centres at points $(0,0)$ and $(0,a)$ we place narrow-band filters with maxima at frequencies $\omega_{0\mathrm{m}}$ and $\omega_{1\mathrm{m}}$, and in the unshaded parts – narrow-band filters with maxima at frequencies $\omega_{0\mathrm{q}}$ and $\omega_{(K/2)\mathrm{q}}$. In the shaded parts of the holes with centres at points $(0,a)$ and $(-a,0)$, we place narrow-band filters with maxima at frequencies $\omega_{2\mathrm{m}}$ and $\omega_{3\mathrm{m}}$, and in the unshaded parts – narrow-band filters with maxima at frequencies $\omega_{+1\mathrm{q}}$ and $\omega_{-1\mathrm{q}}$.

The algorithm for reconstruction of a three-dimensional image of the object consists in constructing K different cross sections of the surface of the object, passing through the centre of gravity of the object C and point A*, optically conjugate with point A, and in finding the distribution of brightness along each of these cross sections. To construct the jth cross section of the object surface, we will form [by rotating the coordinate planes xy, $\delta_x\delta_y$ and f_xf_y around the optical axis of the system (*4*) by the angle $\varphi_j = \pi j/K$] three new coordinate systems with the axes x_j, δ_{jx} and f_{jx} directed along the jth diameter of the screen (*5*). Then, the holes located along the axis δ_{jx}, the photodetectors, mounted in the holes with centres at points $(0,0)$ and $(\mp\delta_{jxn}, 0)$ and recording the time-averaged (T_{s}) intensities $\bar{I}_{\mathrm{iq}}(0,0)$ and $\bar{I}_{\mathrm{iq}}(\mp\delta_{jxn}, 0)$, and the photodetectors, located along the axis f_{jx} on the receiving aperture (*9*) will participate in the reconstruction of the jth cross section passing through the segment CA* (see Fig. 1). In the interference pattern formed by these holes the photodetectors register the intensity distribution

$$I(f_{jx}, t) = |E_{+\mathrm{q}}(f_{jx}, t)\exp(\mathrm{i}\omega_{j\mathrm{q}}t) + E_{\mathrm{qA}}(t)\exp(\mathrm{i}\omega_{0\mathrm{q}}t) + E_{-\mathrm{q}}(f_{jx}, t)\exp(\mathrm{i}\omega_{-j\mathrm{q}}t)|^2,$$

where $\omega_{0\mathrm{q}}$, $\omega_{-j\mathrm{q}}$ and $\omega_{j\mathrm{q}}$ are three frequencies of probe radiation involved in the construction of the jth cross section;

$$E_{\pm\mathrm{q}}(f_{jx}, t) \sim \sum_{n=1}^{N} F_{\mathrm{q}}(\mp\delta_{jxn}, 0)\, u(t - 2r_{\pm jxn}/c) \times \exp[2\pi\mathrm{i}\boldsymbol{r}_{\pm jxn}\boldsymbol{\rho}_{\mathrm{s1}}/(r_{\mathrm{c}}\lambda_{0\mathrm{q}})]\exp[2\pi\mathrm{i}\, V_\perp(\boldsymbol{r}_{\pm jxn})t/\lambda_{0\mathrm{q}}] \times \exp[\pm 2\pi\mathrm{i}\delta_{jxn} f_{jx}/(z_f\lambda_{0\mathrm{q}})];$$

$\boldsymbol{r}_{\pm jxn}$ are the radius vectors of points on the surface of the object, optically coupled with the points $(\pm\delta_{jxn}, 0)$ in its image;

$$E_{\mathrm{qA}}(t) = F_{\mathrm{q}}(0,0)\, u(t - 2r_{\mathrm{A}*}/c)\exp[2\pi\mathrm{i}\boldsymbol{r}_{\mathrm{A}*}\boldsymbol{\rho}_{\mathrm{s1}}/(r_{\mathrm{c}}\lambda_{0\mathrm{q}})] \times \exp[2\pi\mathrm{i}\, V_\perp(\boldsymbol{r}_{\mathrm{A}*})t/\lambda_{0\mathrm{q}}]; \quad (17)$$

$$F_{\mathrm{q}}(\delta_x, 0) = \iint k(x,y)h_{\mathrm{q}}(x,y,\delta_x,0)\exp[2\pi\mathrm{i}q_N\xi(x,y)/\lambda_{0\mathrm{q}}]\,\mathrm{d}x\,\mathrm{d}y.$$

Then, the unit (*8*) under the conditions $\tau_{\mathrm{c}} \ll T_{\mathrm{s}} \ll \lambda_{\mathrm{q}}/(\Omega d_{\mathrm{b}})$, $|\omega_{-j\mathrm{q}} - \omega_{j\mathrm{q}}|\,T_{\mathrm{s}} \gg 1$, $|\omega_{0\mathrm{q}} - \omega_{j\mathrm{q}}|\,T_{\mathrm{s}} \gg 1$ and $\omega_{0\mathrm{q}} \gg |\omega_{0\mathrm{q}} - \omega_{j\mathrm{q}}|$ form the functions $\hat{E}_+$ and $\hat{E}_-$:

$$\hat{E}_{\pm}(f_{jx}) = \frac{1}{T_{\mathrm{s}}}\int_{t_0}^{t_0+T_{\mathrm{s}}} I(f_{jx}, t)\exp[\mathrm{i}(\omega_{\pm j\mathrm{q}} - \omega_{0\mathrm{q}})t]\,\mathrm{d}t \approx \frac{1}{T_{\mathrm{s}}}\int_{t_0}^{t_0+T_{\mathrm{s}}} E_{\pm\mathrm{q}}(f_{jx}, t)\, E^*_{\mathrm{qA}}(t)\,\mathrm{d}t, \quad (18)$$

where

$$E_{\pm\mathrm{q}}(f_{jx}, t) \sim \sum_{n=1}^{N} F_{\mathrm{q}}(\mp\delta_{jxn}, 0)\, u(t - 2r_{\pm jxn}/c) \times \exp[2\pi\mathrm{i}\boldsymbol{r}_{\pm jxn}\boldsymbol{\rho}_{\mathrm{s1}}/(r_{\mathrm{c}}\lambda_{0\mathrm{q}})]\exp[\pm 2\pi\mathrm{i}\delta_{jxn} f_{jx}/(z_f\lambda_{0\mathrm{q}})]; \quad (19)$$

$$E_{\mathrm{qA}}(t) = F_{\mathrm{q}}(0,0)\, u(t - 2r_{\mathrm{A}*}/c)\exp[2\pi\mathrm{i}\boldsymbol{r}_{\mathrm{A}*}\boldsymbol{\rho}_{\mathrm{s1}}/(r_{\mathrm{c}}\lambda_{0\mathrm{q}})].$$

Then, using the square of the modulus of $J_{\mathrm{q}}(s_x)$ of the Fourier transform of the function $\hat{E}_{\pm}(f_{jx})$ and formulas similar to (A1.6) from Appendix 1, we determine, with the help of relations (17)–(19), the heights of the object's surface $Z(\mu\rho_n, \varphi_j) = Z_{+jn} = (L_{\mathrm{c}}/2)\,|B_u(\chi_{+jn})|^{-1}$, $Z_{-jn} = (L_{\mathrm{c}}/2)\,|B_u(\chi_{-jn})|^{-1}$, where $\rho_n = na$; $\chi_{\pm jn} = V_{\mathrm{q}}(Z_{\pm jn})/V_{\pm jn}$; $V_{\mathrm{q}}(Z_{\pm jn})$ are the visibilities of the interference fringes (extracted radiation passing through all the holes) formed by the beams propagating from the fixed hole with the centre at point A and from the holes with centres at points with coordinates $\pm\delta_{jxn}$;

$$V_{+jn} = [\bar{I}_{\mathrm{iq}}(0,0)\,\bar{I}_{\mathrm{iq}}(\rho_n, \varphi_j + \pi)]^{1/2}/[\bar{I}_{\mathrm{iq}}(0,0) + \bar{I}_{\mathrm{iq}}(\rho_n, \varphi_j + \pi)],$$

$$V_{-jn} = [\bar{I}_{\mathrm{iq}}(0,0)\,\bar{I}_{\mathrm{iq}}(\rho_n, \varphi_j)]^{1/2}/[\bar{I}_{\mathrm{iq}}(0,0) + \bar{I}_{\mathrm{iq}}(\rho_n, \varphi_j)];$$

$$\bar{I}_{\mathrm{iq}}(\rho_n, \varphi_j) = \bar{I}_{\mathrm{iq}}(\delta_{jxn}, 0);\ \bar{I}_{\mathrm{iq}}(\rho_n, \varphi_j + \pi) = \bar{I}_{\mathrm{iq}}(-\delta_{jxn}, 0).$$

Taking into account relations (6)–(8) the formulas $L(\mu\rho_n, \varphi_j + \pi) \sim \bar{I}_{\mathrm{iq}}(\rho_n, \varphi_j)$ and $L(\mu\rho_n, \varphi_j) \sim \bar{I}_{\mathrm{iq}}(\rho_n, \varphi_j + \pi)$ that are similar to (A1.7) are used to determine the brightness $L(\mu\rho_n, \varphi_j)$ and $L(\mu\rho_n, \varphi_j + \pi)$ of small sites of the object in the vicinity of its jth cross section, optically conjugate with the image points of the object: $(-\delta_{jxn}, 0) \to (\rho_n, \varphi_j)$ and $(\delta_{jxn}, 0) \to (\rho_n, \varphi_j + \pi)$, $\varphi_j = \pi j/K$. These sites form part of a three-dimensional image of the object, which is concentrated in a small

neighbourhood of the jth cross section of its surface. Similarly, other three-dimensional images of the object are formed, which are concentrated in a small neighbourhood of various cross sections of its surface, starting with the cross section with the number $j = 0$ (cross section P in Fig. 1) and ending with the $K-1$ cross section, i.e., the three-dimensional image of the object is completely reconstructed.

Along with the reconstruction of the three-dimensional image of the object, the unit (*8*) implements the algorithm allowing one to determine three vector components of the angular rotation velocity. To this end, use is made of four holes shown by a triangle on the screen (*5*) and of the probe radiation sources (*1*) and (*14*). When orienting the optical axis of the system (*4*) in the direction of the object and taking into account (*3*) and (*5*) the field recorded by the photodetector (*12*) has the form

$$E_{\rm m}(t) = E_{0\rm m}(t) + E_{1\rm m}(t) + E_{2\rm m}(t) + E_{3\rm m}(t),$$

where

$$E_{k\rm m}(t) \sim \exp(\mathrm{i}\omega_{k\rm m}t)\exp[2\pi\mathrm{i}\boldsymbol{r}_k\boldsymbol{\rho}_{\rm s1}/(r\lambda_{k\rm m})]$$
$$\times \exp[2\pi\mathrm{i}V_\perp(\boldsymbol{r}_k)t/\lambda_{k\rm m}]F_{k\rm m}(\boldsymbol{\delta}_{\perp k});$$
$$\boldsymbol{\delta}_{\perp k} = (\delta_{xk}, \delta_{yk});\ \ k = 0, 1, 2;$$

$$E_{3\rm m}(t) \sim \exp(\mathrm{i}\omega_{3\rm m}t)\exp[2\pi\mathrm{i}\boldsymbol{r}_3\boldsymbol{\rho}_{\rm s2}/(r\lambda_{3\rm m})]$$
$$\times \exp[2\pi\mathrm{i}V_\perp(\boldsymbol{r}_3)t/\lambda_{3\rm m}]F_{3\rm m}(\boldsymbol{\delta}_{\perp 3});$$

$$F_{\nu\rm m}(\boldsymbol{\delta}_\perp) = \iint k(x,y)h_\nu(x,y,\boldsymbol{\delta}_\perp)\exp[2\pi\mathrm{i}q_N\xi(x,y)/\lambda_{\nu\rm m}]\mathrm{d}x\mathrm{d}y;$$
$$\nu = 0, 1, 2, 3;$$

$h_\nu(x,y,\boldsymbol{\delta}_\perp)$ is the pulse response of the system (*4*) at a frequency $\omega_{\nu\rm m}$; $\lambda_{\nu\rm m} = c/\omega_{\nu\rm m}$; $\boldsymbol{\delta}_{\perp 0} = (0,0)$, $\boldsymbol{\delta}_{\perp 1} = (a,0)$, $\boldsymbol{\delta}_{\perp 2} = (0,a)$ and $\boldsymbol{\delta}_{\perp 3} = (-a,0)$ are the coordinates of the centres of the four holes; $\boldsymbol{r}_\nu$ are the radius vectors of points on the object's surface, which are optically conjugate with these centres. Then, at the output of the photodetector (*12*) measuring the intensity $I_{\rm m}(t) = |E_{\rm m}(t)|^2$, the unit (*8*), when the conditions $(\omega_{l\rm m} - \omega_{0\rm m})T_{\rm d} \gg 1$ ($l = 1, 2, 3$) are met, forms three functions that satisfy the relations:

$$S_l(\nu) \sim \frac{1}{T_{\rm d}}\int_{t_0}^{t_0+T_{\rm d}} I_{\rm m}(t)\exp[\mathrm{i}(\omega_{l\rm m} - \omega_{0\rm m})t]\exp(2\pi\mathrm{i}\nu t)\,\mathrm{d}t$$
$$\approx \frac{1}{T_{\rm d}}\int_{t_0}^{t_0+T_{\rm d}} E_{0\rm m}(t)\,E^*_{l\rm m}(t)\exp(2\pi\mathrm{i}\nu t)\,\mathrm{d}t.$$

These functions correspond to the three +1st orders filtered from the spectra of time signals from three interference fringes, each of which is formed due to the interference of the wave propagating from the hole with the centre at point $(0,0)$ with the waves propagating from the holes with centres at points $(a,0)$, $(0,a)$ and $(-a,0)$. When rotating an object, these fringes move along the axes f_x and f_y (Fig. 1). In view of (15) and under conditions

$$\lambda_{0\rm m} \approx \lambda_{l\rm m},$$
$$d_\rho[-\mu\Omega_z a + \Omega_x Z(x=-\mu a, y=0)]T_{\rm d}/(r_{\rm c}\lambda_{0\rm m}) < 0.1, \qquad (20)$$
$$d_\rho\Omega_x Z(x=0, y=-\mu a)T_{\rm d}/(r_{\rm c}\lambda_{0\rm m}) < 0.1$$

the maxima of the filtered +1st orders are calculated on the basis of the relations

$$\nu_1 = 2\mu a\Omega_y/\lambda_{0\rm m},\ \nu_2 = -2\mu a\Omega_x/\lambda_{0\rm m},$$
$$\nu_3 = 2\{-\Omega_y\mu\mathrm{a} + \rho_{\mathrm{s}1y}[-\Omega_z\mu\mathrm{a} + \Omega_x Z(\mu a, 0)]/r_{\rm c}\}/\lambda_{0\rm m},$$

which are used in the unit (*8*) to determine three vector components of the angular rotation velocity $\boldsymbol{\Omega}$ of the object:

$$\Omega_x = -\lambda_{0\rm m}\nu_2/(2\mu a),\ \Omega_y = -\lambda_{0\rm m}\nu_1/(2\mu a),$$
$$\Omega_z = -r_{\rm c}\lambda_{0\rm m}(\nu_3 + \nu_1)/(r_{\mathrm{s}1y}\mu a) + \nu_2\lambda_{0\rm m}Z(\mu a, 0)/[2(\mu a)^2].$$

It should be noted that in determining these components, we simultaneously use the found heights $Z(-\mu a, 0)$, $Z(0,-\mu a)$ and $Z(\mu a, 0)$ of the object's surface at points optically conjugate with points $(a,0)$, $(0,a)$ and $(-a,0)$ in the plane of its image. In this case, the heights $Z(-\mu a, 0)$ and $Z(0,-\mu a)$ are required to check conditions (20) in the unit (*8*), whereas the height $Z(\mu a, 0)$ is needed to determine the component Ω_z of the object.

3. Conclusions

Thus, the paper presents a method which makes it possible to simultaneously form a three-dimensional image and to determine three vector components of the angular rotation velocity of the most remote objects, including near-Earth space objects. First, the method is based on probing the object under study from two directions by multi-frequency laser radiation beams with coherence lengths that are smaller or larger than the object's size and on the formation of a flat image of the object. Secondly, it is based on the use of radially arranged holes in the screen mounted in the region of a flat image of the object, and on the use of the interference fringes formed by radiation beams scattered by an object which pass through these holes.

Appendix 1. Simultaneous determination of height and brightness of the sites of the object's surface located in the vicinity of points A* and B*

The brightness $L(\boldsymbol{r}_{\rm A^*})$ and $L(\boldsymbol{r}_{\rm B^*})$ of small sites of the object, which are located in the vicinity of points A* and B* (Fig. 1), is determined by the photodetectors measuring the time-averaged $[T_{\rm s} \ll \lambda_{0\rm q}/(\Omega d_{\rm b})]$ intensities $\bar{I}_{\rm iq}(\delta_{x\rm A}, \delta_{y\rm A})$ and $\bar{I}_{\rm iq}(\delta_{x\rm B}, \delta_{y\rm B})$ in the image of the object, the photodetectors being placed in the holes with centres at points A and B. In accordance with formulas (6) and (8), $L(\boldsymbol{r}_{\rm A^*}) \sim \bar{I}_{\rm iq}(\delta_{x\rm A}, \delta_{y\rm A})$, $L(\boldsymbol{r}_{\rm B^*}) \sim \bar{I}_{\rm iq}(\delta_{x\rm B}, \delta_{y\rm B})$. Simultaneously, the height $Z_{\rm A^*B^*}$ of point B* is found. To do this, we place in these holes narrow-band filters with maximum transmission at frequencies $\omega_{\rm qA}$ and $\omega_{\rm qB}$ respectively, and probe the object (*2*) by quasi-monochromatic radiation at these frequencies. Let us orient the coordinate system $\delta_x\delta_y$ and $f_x f_y$ (Fig. 1) so that the axis x passed through point B, and the axis f_x was parallel to the axis δ_x. Then, an array of photodetectors located along the axis f_x registers the intensity

$$I_{\rm q}(f_x, t) = |E_{\rm qA}(t)|^2 + |E_{\rm qB}(t)|^2 + H_{\rm AB}(f_x, t)$$
$$\times \exp[\mathrm{i}(\omega_{\rm qA} - \omega_{\rm qB})t] + H^*_{\rm AB}(f_x, t)\exp[\mathrm{i}(\omega_{\rm qB} - \omega_{\rm qA})t],$$

where

$$E_{qA}(t) \sim F_q(0,0)\,u(t - 2r_{A^*}/c)\exp[2\pi i \boldsymbol{r}_{A^*}\boldsymbol{\rho}_{s1}/(r_c\lambda_{qA})],$$

$$E_{qB}(t) \sim F_q(\delta_{xB},0)\,u(t - 2r_{B^*}/c)\exp[2\pi i \boldsymbol{r}_{B^*}\boldsymbol{\rho}_{s1}/(r_c\lambda_{qB})]$$

are the amplitudes of the fields that are generated by the receiving system (*4*) on the holes with centres at points A and B;

$$H_{AB}(f_x,t) = E_{qB}(t)\,E^*_{qA}(t)\exp(2\pi i\delta_{xB}f_x/z_f).$$

Then, the function

$$\hat{E}(f_x) = \frac{1}{T_s}\int_{t_0}^{t_0+T_s} I_q(f_x,t)\exp[-i(\omega_{qA}-\omega_{qB})t]\,dt \qquad (A1.1)$$

is determined in the unit (*8*). Under the conditions

$$T_s \gg \tau_c,\ (\omega_{qA}-\omega_{qB})T_s \gg 1 \text{ и } (\lambda_{qA}-\lambda_{qB})/\lambda_{qA} \ll 1$$

we obtain

$$\hat{E}(f_x) = \frac{1}{T_s}\int_{t_0}^{t_0+T_s} H_{AB}(f_x,t)\,dt = |F_q(0,0)\,F_q(\delta_{xB},0)|$$

$$\times\,|B_u[2(r_{A^*}-r_{B^*})/L_c]|\exp[2\pi i\delta_{xB}f_x/(z_{sc}\lambda_{0q}) + i\psi_{AB}], \qquad (A1.2)$$

where

$$\psi_{AB} = 2\pi(\boldsymbol{r}_{A^*}-\boldsymbol{r}_{B^*})\boldsymbol{\rho}_{s1}/(r\lambda_{0q}) + \arctan\{\mathrm{Re}[F^*_q(0,0)$$

$$\times F_q(\delta_{xB},0)]/\mathrm{Im}[F_q(0,0)\,F^*_q(\delta_{xB},0)]\}.$$

Then, the unit (*8*) determines the square of the modulus of $J_q(s_x)$ of the Fourier transform of the function $\hat{E}(f_x)$

$$G_q(s_x) = (1/d_f)\int \hat{E}(f_x)\exp[2\pi i s_x f_x/(z_f\lambda_{0q})]\,df_x$$

$$= \Theta_+(s_x)\exp(i\psi_{AB})\,|B_u[2Z(-\mu\delta_{xB},0)/L_c]|$$

$$\times\,|F_q(0,0)\,F_q(\delta_{xB},0)|,$$

where d_f is the size of the linear array of the photodetectors (*10*);

$$\Theta_+(s_x) = (1/d_f)\int \exp[2\pi i f_x(\delta_{xB}+s_x)/(z_f\lambda_{0q})]\,df_x,$$

s_x is the spatial coordinate. Using (A1.2) we have

$$J_q(s_x) = |G_q(s_x)|^2 = J_{AB}|\Theta_+(s_x)|^2,$$

where

$$J_{AB} = |G_q(s_x=-\delta_x)|^2 \sim 4|F_q(0,0)\,F_q(\delta_{xB},0)|^2$$

$$\times\,|B_u(2Z_{A^*B^*}/L_c)|^2.$$

Whence, taking into account relations (6) and (8) we obtain the equation

$$|B_u(2Z_{A^*B^*})|^2 = J_{AB}/[4\bar{I}_{iq}(0,0)\,\bar{I}_{iq}(\delta_{xB},0)], \qquad (A1.3)$$

from which it follows that

$$|B_u(2Z_{A^*B^*}/L_c)| = V_q(Z_{A^*B^*})/V_{AB},$$

where

$$V_q(Z_{A^*B^*}) = \sqrt{J_{AB}}/\sqrt{\bar{I}_{iq}(0,0) + \bar{I}_{iq}(\delta_{xB},0)} \qquad (A1.4)$$

is the visibility of the interference fringes formed by beams propagating from the holes with centres at points A and B;

$$V_{AB} = 2\sqrt{\bar{I}_{iq}(0,0)\,\bar{I}_{iq}(\delta_{xB},0)}/[\bar{I}_{iq}(0,0) + \bar{I}_{iq}(\delta_{xB},0)]. \qquad (A1.5)$$

The solution of equation (A1.3) in full accordance with (11) has the form:

$$Z(-\mu\delta_{xB},0) = (L_c/2)\,|B_u(\chi)|^{-1}, \qquad (A1.6)$$

where $\chi = V_q(Z_{A^*B^*})/V_{AB}$. In this case, the brightness of the sites the object's surface, which are located in the vicinity of points A^* and B^* has the form

$$L(\boldsymbol{r}_{A^*}) \sim \bar{I}_{iq}(0,0),\ L(\boldsymbol{r}_{B^*}) \sim \bar{I}_{iq}(\delta_{xB},0). \qquad (П1.7)$$

Appendix 2. Influence of additive noise on the accuracy of determining the heights of the surface of the object under study

We estimate the effect of additive noise on the accuracy of determining the height $Z(-\mu\delta_{xB},0)$, which can be interpreted as a contribution of a flat stationary background object that contains point A^* and is parallel to the receiving aperture (*4*) to the image of the object [4]. In line with this interpretation, in the presence of additive background noise, the field distribution along the axis f_x is

$$E_\Sigma(f_x,t) = E_{A\Sigma}(t)\exp(i\omega_{qA}t)$$

$$+ E_{B\Sigma}(t)\exp[2\pi i\delta_{xB}f_x/(z_{sc}\lambda_{0q})]\exp(i\omega_{qB}t), \qquad (A2.1)$$

where

$$E_{A\Sigma}(t) = E_A(t) + E_{Ap}(t);\ E_{B\Sigma}(t) = E_B(t) + E_{Bp}(t);$$

$$E_{Ap}(t) \sim F_{qp}(0,0)\,u(t - 2z_{A^*}/c)\exp[2\pi i \boldsymbol{r}_{A^*}\boldsymbol{\rho}_{s1}/(r_c\lambda_{qA})];$$

$$E_{Bp}(t) \sim F_{qp}(\delta_{xB},0)\,u(t - 2z_{A^*}/c)\exp[2\pi i \boldsymbol{r}_{B^*}\boldsymbol{\rho}_{s1}/(r_c\lambda_{qB})];$$

$$F_{qp}(\delta_x,0) = \iint k_p(x,y)h_q(x,y,\delta_{xB},0)\exp[2\pi i\xi_p(x,y)/\lambda_{qB}]dx\,dy;$$

$k_p(x,y)$ and $\xi_p(x,y)$ are the distributions of the Fresnel reflection coefficients and the heights of surface roughness of the background object. At the same time, for the background object $|k_p(x,y)|^2 = |k_p(0,0)|^2$ and $\sigma_p = \ell_p$, where σ_p and ℓ_p are the rms deviation and correlation radius of the distribution $\xi_p(x,y)$. In the presence of additive noise the array of photodetectors, which is located along the axis f_x (Fig. 1), registers the intensity

$$I_{q\Sigma}(f_x,t) = |E_{q\Sigma}(f_x,t)|^2 \sim |E_{qA\Sigma}(t)|^2 + |E_{qB\Sigma}(f_x,t)|^2$$

$$+ H_{AB\Sigma}(f_x,t)\exp[i(\omega_{qA}-\omega_{qB})t]$$

$$+ H^*_{AB\Sigma}(f_x,t)\exp[i(\omega_{qB}-\omega_{qA})t], \qquad (A2.2)$$

where $H_{AB\Sigma}(f_x,t) = E_{B\Sigma}(f_x,t)\,E^*_{A\Sigma}(t)$. Then, in the presence of noise the unit (*8*) determines the function

$$\hat{E}_\Sigma(f_x) = \frac{1}{T_s}\int_{t_0}^{t_0+T_s} I_{q\Sigma}(f_x,t)\exp[-i(\omega_{qA}-\omega_{qB})t]\,dt.$$

Given that $(\omega_{qA}-\omega_{qB})T_s \gg 1$ and the additive noise is statistically independent of the useful signal, we obtain

$$\hat{E}_\Sigma(f_x) \approx \frac{1}{T_s}\int_{t_0}^{t_0+T_s} H_{AB\Sigma}(f_x,t)\,dt \sim |F_q(0,0)\,F_q(\delta_{xB},0)| \times |B_u[2(r_{A^*}-r_{B^*})/L_c]|\exp[2\pi i\delta_{xB}f_x/(z_f\lambda_{0q}) + i\psi_{AB}] + |F_{qp}(0,0)\,F_{qp}(\delta_{xB},0)|\exp[2\pi i\delta_{xB}f_x/(z_f\lambda_{0q}) + i\psi_{ABp}],$$

where

$$\psi_{ABp} = 2\pi(\boldsymbol{r}_{A^*}-\boldsymbol{r}_{B^*})\boldsymbol{\rho}_{s1}/(r\lambda_{0q}) + \arctan\{\mathrm{Re}[F^*_{qp}(0,0) \times F_{qp}(\delta_{xB},0)]/\mathrm{Im}[F_{qp}(0,0)\,F^*_{qp}(\delta_{xB},0)]\}.$$

Under the same conditions, taking into account relation (A2.2) the square of the modulus of the Fourier transform of the function $\hat{E}(f_x)$ is $J_{q\Sigma}(s_x) = (J_{AB}+J_{ABp})|\Theta_+(s_x)|^2$, where $J_{ABp} \sim 4|F_{qp}(0,0)\,F_{qp}(\delta_{xB},0)|^2$. In accordance with (A1.3) the estimate $\tilde{Z}$ of the height $Z(-\mu\delta_{xB},0)$ of the object's surface at point B* is determined from the equation

$$|B_u[2\tilde{Z}(-\mu\delta_{xB},0)/L_c]|^2 = (J_{AB}+J_{ABp})/[4\bar{I}_\Sigma(\delta_{xB},0)\,\bar{I}_\Sigma(0,0)],$$

where $\bar{I}_\Sigma(0,0) = \bar{I}_{iq}(0,0) + \bar{I}_{iqp}(0,0)$ and $\bar{I}_\Sigma(\delta_{xB},0) = \bar{I}_{iq}(\delta_{xB},0) + \bar{I}_{iqp}(\delta_{xB},0)$ are the signals recorded by the photodetectors placed in the holes with centres at points A and B; taking into account relations (A2.1) and (8),

$$\bar{I}_{iqp}(\delta_{xB},0) = \frac{1}{T_s}\int_{t_0}^{t_0+T_s}|E_{iqp}(t,\delta_{xB},0)|^2\,dt \sim |F_{qp}(\delta_{xB},0)|^2 \sim |k_p(\delta_{xB},0)|^2 \qquad (A2.3)$$

is the time-averaged (T_s) intensity of the image of the background object. Under the conditions $\bar{I}_{iqp}(0,0) \ll \bar{I}_{iq}(0,0)$ and $\bar{I}_{iqp}(\delta_{xB},0) \ll \bar{I}_{iq}(\delta_{xB},0)$ we have

$$\langle|B_u[2\tilde{Z}(-\mu\delta_{xB},0)/L_c]|^2\rangle_p \approx |B_u[2Z(-\mu\delta_{xB},0)/L_c]|^2 + \langle\bar{I}_{iqp}(\delta_{xB},0)\,\bar{I}_{iqp}(0,0)\rangle_p/[\bar{I}_{iq}(\delta_{xB},0)\,\bar{I}_{iq}(0,0)], \qquad (A2.4)$$

where the angle brackets $\langle\ldots\rangle_p$ denote averaging over different realisations of the background noise.

On the other hand, approximating the function $|B_u(z)|^2$ by the Gaussian function, at small deviations ΔZ of the estimate $\tilde{Z}$ from $Z(-\mu\delta_{xB},0)$, we obtain

$$|B_u[2\tilde{Z}(-\mu\delta_{xB},0)/L_c]|^2 \approx |B_u[2Z(-\mu\delta_{xB},0)/L_c]|^2 + [(\Delta Z)^2/2](d^2|B_u[2Z(-\mu\delta_{xB},0)/L_c]|^2/dZ^2), \qquad (A2.5)$$

where $\Delta Z = \tilde{Z} - Z(-\mu\delta_{xB},0)$; $d^2|B_u[2Z(-\mu\delta_{xB},0)/L_c]|^2/dZ^2 \approx 1/L_c^2$. Under the assumption that $\langle\Delta Z\rangle_p = 0$ and taking into account relations (A2.4), (A2.5) for the rms deviation evaluation of the height $Z(-\mu\delta_{xB},0)$, we have the expression

$$\sigma_p = \langle(\Delta Z)^2\rangle_p^{1/2} \approx 1.4L_c\frac{\langle\bar{I}_{iqp}(\delta_{xB},0)\,\bar{I}_{iqp}(0,0)\rangle_p^{1/2}}{[\bar{I}_{iq}(\delta_{xB},0)\,\bar{I}_{iq}(0,0)]^{1/2}}.$$

Finally, taking into account relations (8), (A2.1) and (A2.2) we obtain

$$\sigma_p \approx 1.4L_c\langle|k_p(0,0)|^4\rangle_p^{1/2}/[k_{iq}(\delta_{xB},0)\,k_{iq}(0,0)]^{1/2}.$$

The relative accuracy of determining the height is $\eta_p = \sigma_p/Z(-\mu\delta_{xB},0)$. For point B*, located near the centre of the backscattering region of the object (point A* in Fig. 1), $k_{iq}(\delta_{xB},0) \approx k_{iq}(0,0)$ and $\sigma_p \approx \sigma_{p1} = 1.4L_c\langle|k_p(0,0)|^4\rangle_p^{1/2}/k_{iq}(0,0)$, while $\eta_p \approx 1.4[L_c/Z(-\mu\delta_{xB},0)]\langle|k_p(0,0)|^4\rangle_p^{1/2}/k_{iq}(0,0)$. Change in the parameters σ_p and η_p when moving point B* away from point A* is most clearly demonstrated by an object with a spherical shape of the surface. Then, $k_{iq}(\delta_{xB},0) \approx k_{iq}(0,0)\times\exp\{-[\delta_{xB}\ell_\xi/(\rho_0\sigma_\xi)]^2\}$ and the accuracy of determining the height $Z(-\mu\delta_{xB},0)$ when approaching the edge of the backscattering region $\delta_{xB} \approx \rho_0[\sigma_\xi/(2\ell_\xi)]$ is reduced due to the increase in the parameter σ_p, which reaches $\sigma_{p2} = 10\sigma_{p1}$. In this case, the relative accuracy of determining the height varies from $\eta_{p1} \approx \sigma_{p1}/Z_1$ to $\eta_{p2} \approx \sigma_{p2}/Z_2$, where $Z_1 = a^2/(2\rho_0)$ is the height nearest to point A*; $a = \lambda_q d_\rho/z_{sc}$ is the size of a speckle in the image of the object; $Z_2 = h_b \approx \rho_0[\sigma_\xi^2/(2\ell_\xi^2)]$.

References

1. Leith E.N., Upatnieks J. *J. Opt. Soc. Am.*, **52**, 522 (1962).
2. Denisyuk N. *Opt. Spektrosk.*, **15**, 522 (1963).
3. Dubnishchev Yu.N. et al. *Opt. Spektrosk.*, **34**, 587 (1973).
4. Bakut P.A., Mandrosov V.I., Matveev I.N., Ustinov N.D. *Teoriya kogerentnykh izobrazhenii* (The theory of Coherent Images) (Moscow: Radio i svyaz', 1987).
5. Mandrosov V. *Coherent Fields and Images in Remote Sensing* (Bellingham, Wash.: SPIE Press, 2004) Vol. PM130.
6. Mandrosov V.I. *Kvantovaya Elektron.*, **39**, 1059 (2009) [*Quantum Electron.*, **39**, 1059 (2009)].
7. Mandrosov V.I. *Kvantovaya Elektron.*, **41**, 179 (2011) [*Quantum Electron.*, **41**, 179 (2011)].
8. Bakut P.A., Mandrosov V.I. *Kvantovaya Elektron.*, **36**, 239 (2006) [*Quantum Electron.*, **36**, 239 (2006)].
9. Goodman J. *Statistical Optics* (New York: Wiley, 1985; Moscow: Mir, 1986).